nature geoscience

LETTERS

PUBLISHED ONLINE: 24 MARCH 2013 | DOI: 10.1038/NGEO1770

The long precursory phase of most large interplate earthquakes

Michel Bouchon[1]*, Virginie Durand[1,2]*, David Marsan[2], Hayrullah Karabulut[3] and Jean Schmittbuhl[4]

Many earthquakes are preceded by foreshocks[1,2]. However, the mechanisms that generate foreshocks and the reason why they occur before some earthquakes and not others are unknown[3–8]. Here we use seismic catalogues from the best instrumented areas of the North Pacific to analyse the foreshock sequences preceding all earthquakes there between 1999 and 2011, of magnitude larger than 6.5 and at depths shallower than 50 km. The data set comprises 31 earthquakes at plate boundaries, and 31 in plate interiors. We find that there is a remarkable contrast between the foreshock sequences of interplate compared with intraplate earthquakes. Most large earthquakes at plate interfaces in the North Pacific were preceded by accelerating seismic activity in the months to days leading up to the mainshock. In contrast, foreshocks are much less frequent in intraplate settings. We suggest that at plate boundaries, the interface between the two plates begins to slowly slip before the interface ruptures in a large earthquake. This relatively long precursory phase could help mitigate earthquake risk at plate boundaries.

Foreshocks are the most common precursory phenomenon to earthquakes. However, they have proved elusive to predict them. The inherent problem is the difficulty to identify seismic events as foreshocks when they occur. The view that foreshocks are of little use to predict earthquakes is supported by models where foreshocks trigger one another, and one of them randomly triggers the mainshock. However, such models are contradicted by investigations of well-recorded foreshock sequences[8–12] that suggest instead that their source is aseismic fault slip—slip too slow to radiate seismic waves—foreshocks resulting from the breaking of the asperities of the fault plane resisting the slow slip of the surrounding areas. Recent observations of foreshock sequences before the giant M_w 9.0 Tohoku, Japan earthquake[13] and the large M_w 7.6 Izmit, Turkey earthquake[14] indicate that their rupture was preceded by a phase of slow slip of the plate interface. Whereas the Tohoku earthquake broke the interface between a subducting plate and the overriding one, the Izmit event occurred between two horizontally moving plates. They represent the two types of large interplate earthquake: subduction and transform. Although neighbouring plates slip continuously over most of their contact interface, because rocks at depth are ductile enough to slowly deform, the shallow part of their interface is generally locked for long times until rocks suddenly break in an earthquake. Another type of earthquake, termed intraplate, results from the internal deformation of a plate.

Observations made over the past decade have shown that besides the continuous and the earthquake modes, relative plate motion may occur in a variety of ways[15–17]: slow-slip events lasting for weeks or months occurring below the locked seismogenic zone of subductions, hours-long tremors originating from below the seismogenic zone along both subducting and transform boundaries, slow post-seismic slip following large earthquakes and partly occurring within the seismogenic zone. Geodetic measurements also show that earthquakes cannot account for all of the slip that takes place in subduction seismogenic zones[18], implying that some slip must occur aseismically. These observations show that slow slip is a significant mode of relative plate motion and is pervasive in the seismogenic zone itself. Thus, if a link between foreshocks and slow slip exists, as has long been proposed[2,8–11,13,14,19], foreshocks may be more common before interplate than intraplate earthquakes.

One challenge of comparing foreshock occurrences over wide geographic areas is the heterogeneity of magnitude detection thresholds, which is related to the density of seismic stations. As some foreshock sequences may not contain events large enough to be detected at far distance, one must rely on capabilities of regional networks. Thus, we will focus on what may be the world's best instrumented seismic zones: the zone extending from southern Taiwan to northern Japan and the one stretching from western Alaska to northern Mexico (Fig. 1). We will consider all of the $M \geq 6.5$ earthquakes shallower than 50 km that occurred there between 1 January 1999 and 1 January 2011. Excluding events that are early aftershocks of larger events (Supplementary Section S1), this provides a set of 62 $M \geq 6.5$ earthquakes (Fig. 1 and Supplementary Tables S1–S3), which divides evenly into 31 interplate (22 subductions and 9 transforms) and 31 intraplate earthquakes. The analysis of the data set (Supplementary Fig. S1) shows that the magnitude of completeness is about 2.5 for both interplate and intraplate seismicity.

For each event, we investigate the evolution of seismicity in a zone of 50 km radius centred on the epicentres. The choice of this radius is based on the observation that the clearest foreshock sequences of the data set have more than 98% of their pre-earthquake events in this range (Supplementary Section S1). As shown later, this choice is not critical to the study. Figure 2 shows that an acceleration of activity precedes on the last day most of the interplate earthquakes of the data set. This figure presents all of the interplate sequences with last-day events (~70% of the total). It shows that for most of the interplate earthquakes, the largest event of the last 4 days occurs on the last day, generally in the last hours before the earthquake. The 5 sequences of Fig. 2a for which the largest event is not on the last day have, nevertheless, most of their last-day seismicity concentrated in the last 4 h (Fig. 2b), indicating also an intensification of the activity. Evolutions over different

[1]Centre National de la Recherche Scientifique and Université Joseph Fourier, Grenoble, ISTerre, BP 53, 38041 Grenoble, France, [2]Université de Savoie, ISTerre, 73376 Le Bourget du Lac, France, [3]Kandilli Observatory and Earthquake Research Institute, Bogaziçi University, KOERI, 81220 Cengelköy, Istanbul, Turkey, [4]Centre National de la Recherche Scientifique and Université de Strasbourg, EOST, 5 rue Descartes, 67084 Strasbourg, France.
*e-mail: Michel.Bouchon@ujf-grenoble.fr; Virginie.Durand@ujf-grenoble.fr.

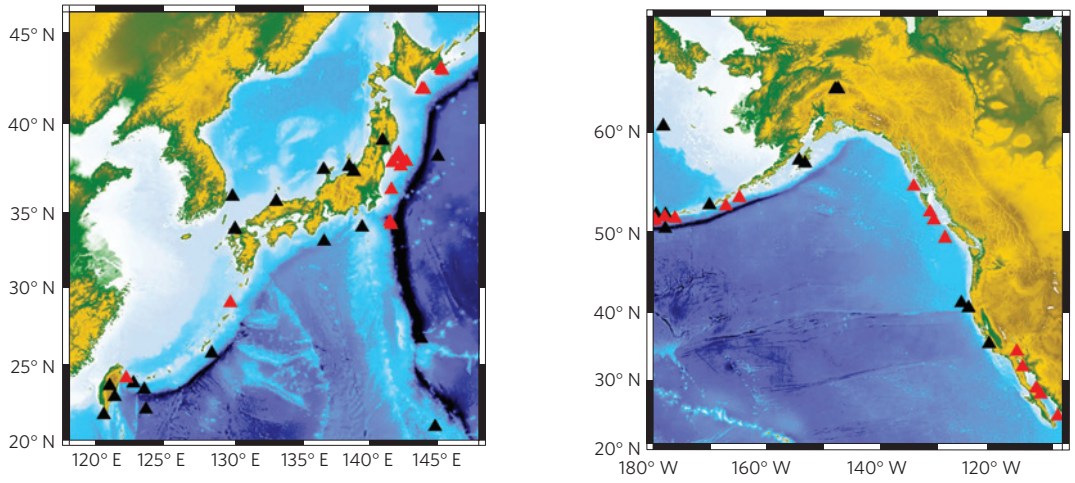

Figure 1 | Geographical distribution of the earthquakes. All of the $M \geq 6.5$ earthquakes (interplates in red; intraplates in black) that occurred between 1 January 1999 and 1 January 2011 in the two zones considered are shown, except those that are early aftershocks of larger events.

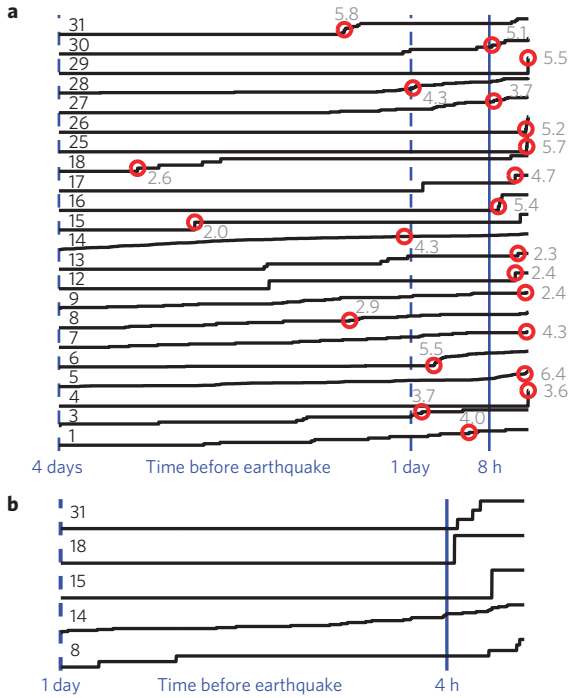

Figure 2 | Evolution of the cumulative numbers of events in the few days before 22 interplate earthquakes (~70% of the data set). All of the events located within 50 km of each interplate earthquake epicentre are included. Bold numbers identify earthquakes in Supplementary Table S1. All curves are normalized and end before the earthquake. **a**, Last 4 days' evolution. Red circles indicate the largest events of the period with their magnitude. **b**, Zoom on the last-day evolution of the 5 sequences of **a** for which the largest event is not on the last day. One of the sequences shown (14) is contaminated by aftershocks of a previous earthquake (see Supplementary Table S1), but shows nevertheless an acceleration in the few hours before the earthquake (see also Supplementary Fig. S9, top trace).

periods (Supplementary Figs S2–S9) show that the acceleration is not restricted to the last day.

As the strength of a seismic source is measured by its seismic moment, we present the pre-earthquake evolution of the moment released in the 50 km zone surrounding the epicentre of most interplate earthquakes (Fig. 3a). Different time windows are considered, because the timing of an eventual acceleration may differ. Although 6 sequences are not shown because they lack a clear trend, the remaining 25 sequences (~80% of the total) show that a notable increase in released seismic moment occurs before the earthquakes. As the timing of the increase varies, one might argue that it is an artefact of the multiple-window presentation[20]. A stack of the seismic moments of all the interplate sequences (Fig. 3b–d) shows that the increase viewed in the individual sequences is real and provides an average picture of the accelerating seismicity. It shows a near-constant seismicity rate until about 2 months before the earthquakes when a small increase becomes noticeable. About 20 days before, the increase becomes more pronounced. The rate accelerates about 2 days before the earthquakes, and again a few hours before, and keeps accelerating until the earthquakes. These plots, like the original acceleration curves of ref. 1, provide a smooth average representation of a process that is more irregular for each event. Nevertheless, they indicate that the acceleration phase that precedes many large interplate earthquakes is remarkably robust and that its timing and duration are surprisingly recurrent. Its presence is insensitive to the assumed size of the foreshock zone (Supplementary Fig. S10).

The pattern of seismicity increase is far less common for intraplate earthquakes. Analysing the last few days' evolution (Supplementary Fig. S11) shows that only 5 sequences (16%) have the largest event of the last 4 days occurring within the 8 h preceding the earthquake compared with 42% for interplate sequences (Fig. 2a). This is confirmed by a comparison of the stacks (Fig. 4a,b). To quantify the difference, we use a simple statistical tool that compares the number of events in successive time windows (Supplementary Section S4). Each 6-month-long pre-earthquake sequence is tested against 1,000 realizations of random sequences containing the same number of events, and the probability that the acceleration observed is not due to chance is calculated. The results (Fig. 4c,d) show that whereas 67% of interplate sequences exhibit an acceleration of seismicity with a probability higher than 70% that it is not due to chance, this number is only 23% for intraplate sequences. In a further test, we also apply the above algorithm to the period starting one year before the earthquake and ending 6 months before. The results (Supplementary Fig. S12) show that in this period, only 23% of interplate sequences reach the probability level defined above.

As seismic events tend to cluster in space and time, one may wonder whether the observed acceleration is not a result of it. Earthquake clustering causes an acceleration of seismicity before a mainshock[21]. As earthquakes trigger aftershocks, the probability of an event is greater following a large shock, when the seismicity rate is

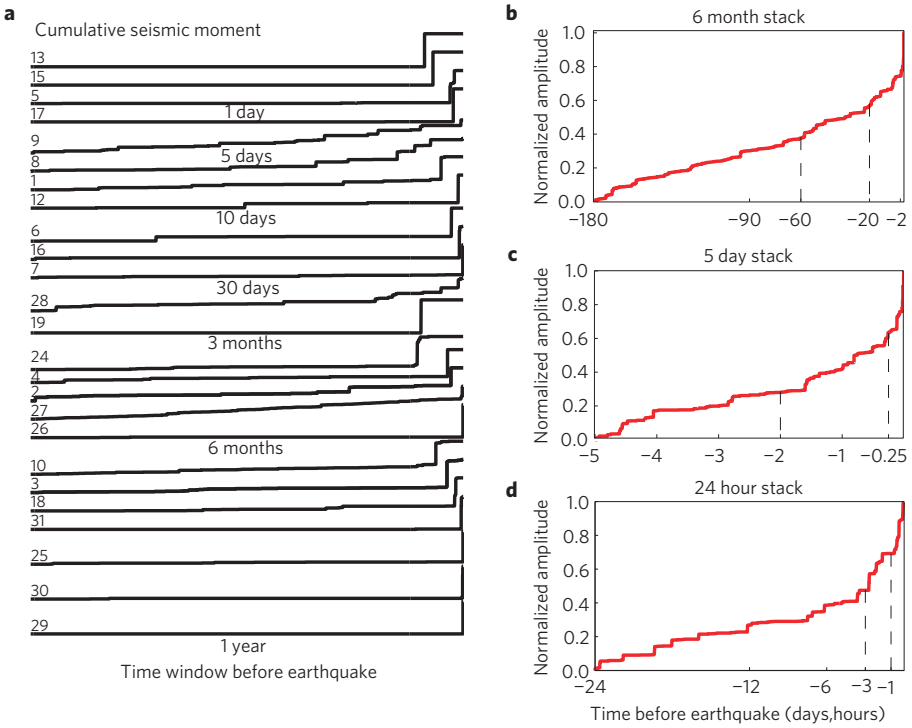

Figure 3 | Time evolution of the seismic moment released in the 50-km-radius zone surrounding the epicentre before interplate earthquakes. **a**, Normalized cumulative moment for 25 pre-earthquake sequences (~80% of the total data set). Numbers at the left identify the sequences in Supplementary Table S1. Time-window lengths are indicated below each set of traces. The magnitude of the largest event of each trace is listed in Supplementary Table S1. **b**–**d**, Normalized stacks of the cumulative seismic moments of all the interplate sequences. Each sequence carries the same weight. Vertical dashed lines refer to numbers below.

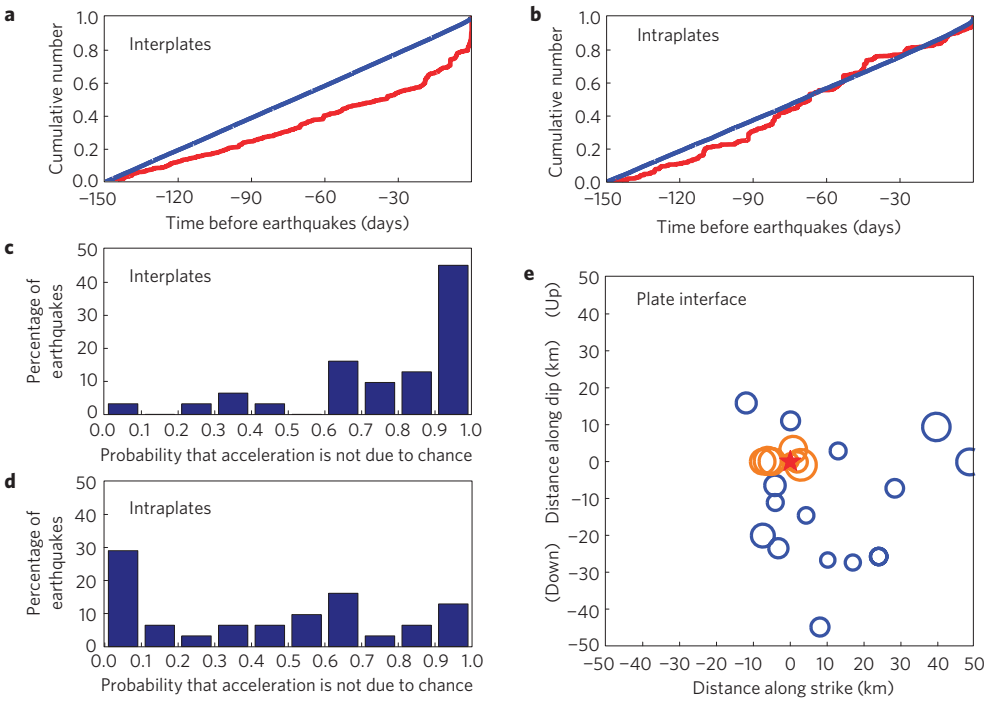

Figure 4 | Comparison of the characteristics of the different types of pre-earthquake sequence. **a**,**b**, Normalized stacked evolution of seismicity (in red) before the interplate and intraplate earthquakes. Every sequence carries the same weight. The blue curve shows the corresponding epidemic-type aftershock sequence simulation. **c**,**d**, Probability that the acceleration of seismicity observed before large earthquakes is not due to chance. **e**, Location of the last event before the 22 interplate earthquakes with last-day event (Fig. 2) relative to the mainshock hypocentre. The map shows the projection of the catalogue location on the plate interface and is centred on the earthquake hypocentre (red star). Subduction is in blue; transform in orange. Symbol size varies linearly with magnitude, which ranges from 1.5 to 5.5.

high. Immediately before the event, there are thus a greater number of earthquakes than normal, causing an apparent acceleration. To estimate how much this statistical (rather than mechanical) acceleration contributes to our observations, we perform two different tests. First, we choose one event in each sequence, which takes place at least 3 months before the $M \geq 6.5$ earthquake and is located close to it, and stack the seismicity of all the sequences relatively to the occurrence time and location of these selected events. The resulting graph (Supplementary Fig. S13) shows that the acceleration due to clustering is very small. In a second test, we perform Monte Carlo simulations of an epidemic-type aftershock sequence model[22] for the 62 sequences (Supplementary Section S5 and Fig. S14). The results (Fig. 4a) show that, although the clustering causes a purely statistical acceleration of seismicity before the earthquakes (Supplementary Fig. S15), it contributes little to the actual acceleration.

The spatial distribution of foreshocks may also shed light on their generating mechanism. Figure 4e shows the locations of the last shock of the 22 interplate sequences of Fig. 2 and suggests different patterns for subduction and transform-fault foreshocks. While the former ones define a broad area and occur relatively far from the hypocentre (∼25 km on average), the later ones cluster close to it (∼4 km on average). Although location errors are probably higher for subduction earthquakes, which generally occur further from land, the difference seems large enough (the average distance for subduction is about 10 times the catalogue-reported location errors, Supplementary Section S6) to reflect mechanical differences. The average magnitude of the immediate subduction foreshocks is 2.6, which, assuming a typical stress drop of ∼3 MPa, implies an average source size of ∼250 m. As this value is 100 times smaller than the average foreshock–mainshock distance and as seismic events do not generally trigger seismicity beyond about twice their source size, the observed pattern seems to preclude triggering of the mainshock by foreshocks for most of the subduction earthquakes of the data set. It suggests a mechanical process that involves at the same time a relatively broad area of the subducting interface. One possible mechanism would be the slow slip of a patch of the subducting plate before the earthquake. In this case, foreshocks would be produced by the breaking of frictional asperities resisting slip. The relatively large extent of subduction foreshock zones suggested by Fig. 4e agrees with what is observed before the M 9.0 March 2011 Japan Tohoku earthquake[13], the 2010 M 8.8 Chile Maule earthquake[23] and the largest ever recorded earthquake, the 1960 M 9.5 Chile earthquake[24]. The clustering of foreshocks around the hypocentre of transform-fault earthquakes, on the other hand, agrees with the few well-resolved studies of such sequences[9–12,14]. The closeness of the locations, of the order of the catalogue error, prevents further investigation. However, the few detailed observations reported show that relative locations generally preclude foreshock-to-foreshock triggering[9–12,14].

The present observations show that most interplate earthquakes are preceded by a phase of increased seismic activity, for which a possible mechanism is the slow slip of the plate interface. At the present resolution of seismic networks, this phase seems less common before intraplate earthquakes, suggesting differences in the mechanical processes leading to rupture. The high probability that large interplate earthquakes are preceded by a phase of accelerating seismicity should motivate denser instrumental deployment along sensitive plate boundaries. Whether such phases also occur without triggering a large event needs investigation.

Received 10 September 2012; accepted 13 February 2013; published online 24 March 2013

References

1. Jones, L. M. & Molnar, P. Frequency of foreshocks. *Nature* **262,** 677–679 (1976).
2. Jones, L. M. & Molnar, P. Some characteristics of foreshocks and their possible relationship to earthquake prediction and premonitory slip on faults. *J. Geophys. Res.* **84,** 3596–3608 (1979).
3. Abercrombie, R. E. & Mori, J. Occurrence patterns of foreshocks to large earthquakes in the western United States. *Nature* **381,** 303–307 (1996).
4. Reasenberg, P. A. Foreshock occurrence before large earthquakes. *J. Geophys. Res.* **104,** 4755–4768 (1999).
5. Jones, L. M. Foreshocks (1966–1980) in the San Andreas system, California. *Bull. Seismol. Soc. Am.* **74,** 1361–1380 (1984).
6. Doser, D. I. Foreshocks and aftershocks of large ($M > 5.5$) earthquakes within the western Cordillera of the United States. *Bull. Seismol. Soc. Am.* **80,** 110–128 (1990).
7. Maeda, K. Time distribution of immediate foreshocks obtained by a stacking method. *Pure Appl. Geophys.* **155,** 381–394 (1999).
8. McGuire, J. J., Boettcher, M. S. & Jordan, T. H. Foreshock sequences and short-term earthquake predictability on East Pacific rise transform faults. *Nature* **434,** 457–461 (2005).
9. Dodge, D. A., Beroza, G. C. & Ellsworth, W. L. Foreshock sequence of the 1992 Landers, California, earthquake and its implications for earthquake nucleation. *J. Geophys. Res.* **100,** 9865–9880 (1995).
10. Dodge, D. A., Beroza, G. C. & Ellsworth, W. L. Detailed observations of California foreshock sequences: Implications for the earthquake initiation process. *J. Geophys. Res.* **101,** 22371–22392 (1996).
11. Zanzerkia, E. E., Beroza, G. C. & Vidale, J. E. Waveform analysis of the 1999 Hector Mine foreshock sequence. *Geophys. Res. Lett.* **30,** 1429 (2003).
12. Hauksson, E. *et al.* The 2010 Mw 7.2 El Mayor-Cucapah earthquake sequence, Baja California, Mexico and southernmost California, USA: Active seismotectonics along the Mexican Pacific margin. *Pure Appl. Geophys.* **168,** 1255–1277 (2011).
13. Kato, A., Obara, K., Igarashi, T., Tsuruoka, H., Nakagawa, S. & Hirata, N. Propagation of slow slip leading up to the 2011 Mw 9.0 Tohoku-Oki earthquake. *Science* **335,** 705–708 (2012).
14. Bouchon, M., Karabulut, H., Aktar, M., Ozalaybey, S., Schmittbuhl, J. & Bouin, M.P. Extended nucleation of the 1999 Mw 7.6 Izmit earthquake. *Science* **331,** 877–880 (2011).
15. Peng, Z. & Gomberg, J. An integrated perspective of the continuum between earthquakes and slow-slip phenomena. *Nature Geosci.* **3,** 599–607 (2010).
16. Beroza, G. C. & Ide, S. Slow earthquakes and nonvolcanic tremor. *Annu. Rev. Earth Planet. Sci.* **39,** 271–296 (2011).
17. Vidale, J. E. & Houston, H. Slow slip: A new kind of earthquake. *Phys. Today* **65,** 38–43 (2012).
18. Pacheco, J., Sykes, L. R. & Scholz, C. H. Nature of seismic coupling along simple plate boundaries of subduction type. *J. Geophys. Res.* **98,** 14133–14159 (1993).
19. Ohnaka, M. Earthquake source nucleation: A physical model for short term precursors. *Tectonophysics* **211,** 149–178 (1992).
20. Hardebeck, J. L., Felzer, K. & Michael, A. J. Improved tests reveal that the accelerating moment release hypothesis is statistically insignificant. *J. Geophys. Res.* **113,** B08310 (2008).
21. Helmstetter, A., Sornette, D. & Grasso, J. R. Mainshocks are aftershocks of conditional foreshocks: How do foreshock statistical properties emerge from aftershock laws. *J. Geophys. Res.* **108,** 2046 (2003).
22. Ogata, Y. Statistical models for earthquake occurrence and residual analysis for point processes. *J. Am. Stat. Assoc.* **83,** 9–27 (1988).
23. Madariaga, R., Métois, M., Vigny, C. & Campos, J. Central Chile finally breaks. *Science* **328,** 181–182 (2010).
24. Suyehiro, S. Difference between aftershocks and foreshocks in the relationship of magnitude to frequency of occurrence for the great Chilean earthquake of 1960. *Bull. Seismol. Soc. Am.* **56,** 185–200 (1966).

Acknowledgements

We thank J. R. Grasso, M. Campillo, F. Renard, P. Y. Bard, M. P. Bouin, O. Coutant, P. Bernard, L. Géli, P. Henry, R. Archuleta, O. Lengliné and G. Poupinet for discussions.

Author contributions

M.B. and V.D. analysed the data and investigated the time and space evolutions. D.M. developed and performed the statistical analysis, H.K. and J.S. investigated the characteristics of the precursory phase. All authors contributed to the conclusions presented in the manuscript.

Additional information

Supplementary information is available in the online version of the paper. Reprints and permissions information is available online at www.nature.com/reprints. Correspondence and requests for materials should be addressed to M.B. or V.D.

Competing financial interests

The authors declare no competing financial interests.